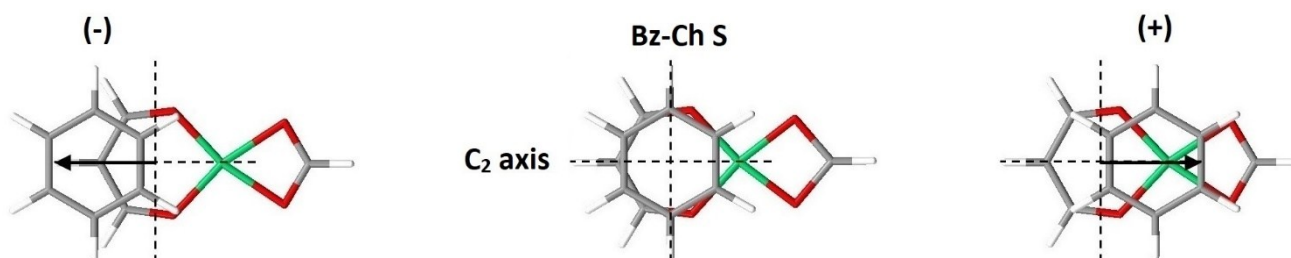


## SUPPORTING INFORMATION

### Potential energy curves for chelate-aryl stacking

The *acac*-type monomers were optimized in Gaussian 09 (version D.01) using the  $\omega$ B97X-D method and aug-cc-pVDZ basis set,<sup>1</sup> while the nickel *dt* monomer was optimized using the B2PLYP-D3BJ method and def2-TZVP basis set.<sup>2</sup> We have then calculated potential energy surfaces for the chelate-aryl stacking interactions of six-membered *acac*-type chelate rings of Ni, Cu and Zn, and of *dt* chelate ring of Ni, by changing the normal distances for a series of offset values (Figure 3 in the main text). These calculations were performed using the  $\omega$ B97X-D density functional with def2-TZVP basis set for *acac*-type chelates and 6-31+G\* basis set for *dt* chelate, since it was shown that they are in good agreement with the gold standard CCSD(T)/CBS level for chelate-aryl stacking interactions.



**Figure S1.** Benzene-chelate sandwich geometry (**Bz-Ch S**) for the calculations of potential energy surfaces has benzene ring center exactly above the chelate ring center. The potential surfaces are calculated by varying the normal distances for the series of offset values. In all calculations the interplanar angle between the rings is  $0^\circ$ . The offsets are denoted negative (-) if benzene is displaced away of the metal, and positive (+) if benzene is displaced towards the metal.

Potential energy curves show the energies of the optimal normal distance at each offset value (Figure S2). They reveal two minimum geometries (Figures 1 and 2 in the main text). In the first one (**Bz-Ch min1**), benzene center is located above the area of C2 atom of the interacting chelate (Figures 1 and 2). In the other geometry (**Bz-Ch min2**), benzene center is above the metal area of the chelate (Figures 1 and 2). For the purpose of the SAPT energy decomposition analysis, the more precise geometries of the sandwich orientation (**Bz-Ch S**, Figure S3) and the geometries of minima (**Bz-Ch min1** and **Bz-Ch min2**, Figures 1 and 2) for chelate-aryl stacking interactions were determined. It was done by performing more detailed scan of potential energy surface, with 0.1 Å step for offset and 0.01 Å step for normal distance. The geometrical parameters and the energies for the curve minima are presented in the main text of this work, while the data for sandwich orientation are given here.

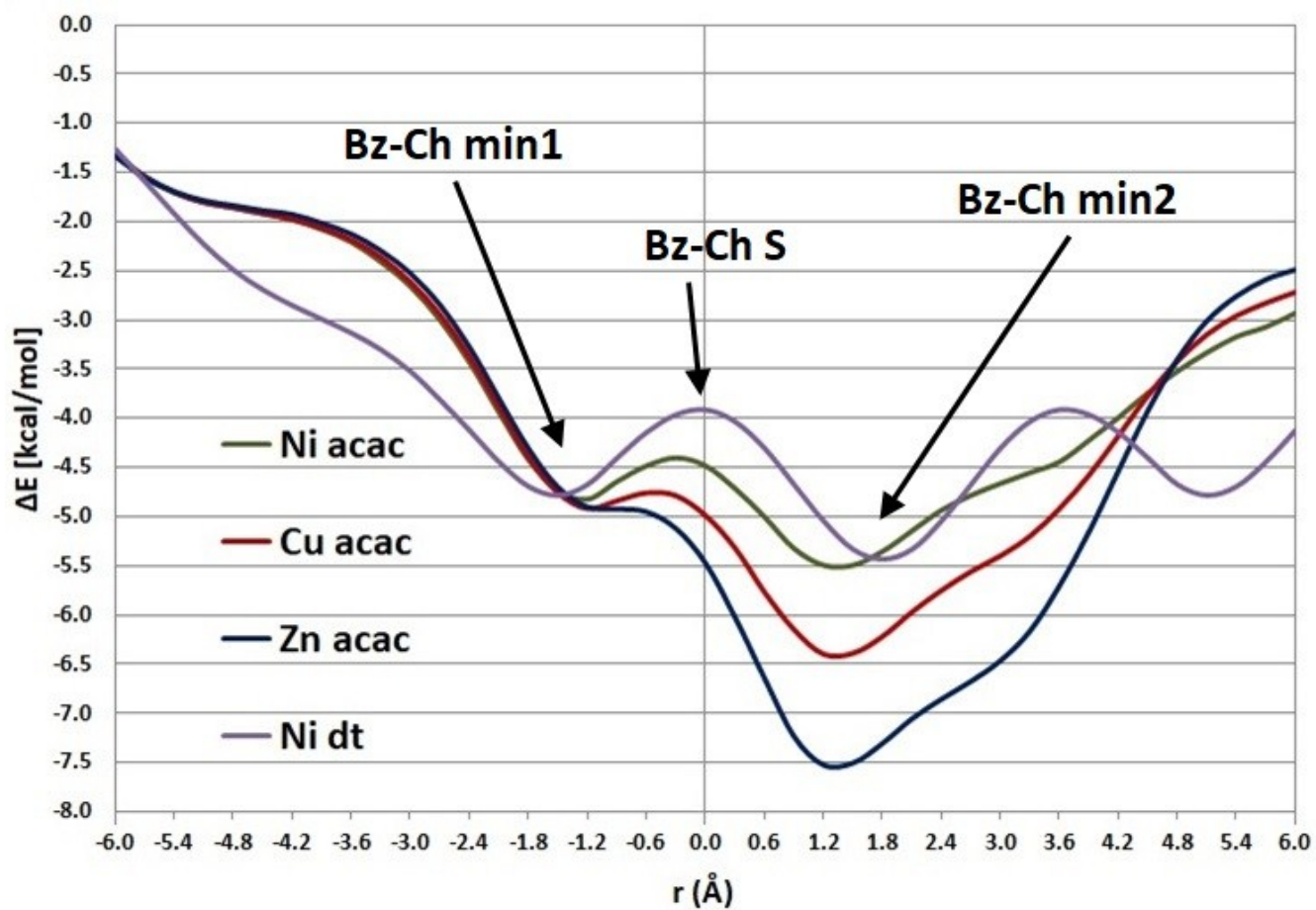


**Figure S2.** Potential energy curves for chelate-aryl stacking calculated with  $\omega$ B97X-D method. The def2-TZVP basis set was used for *acac*-type chelates, while 6-31+G\* basis set was used for dithiolene (*dt*) chelates. The curves were obtained by varying the normal distances for a series of offset values and they show the energies of the strongest interactions for all offsets. The geometries of the minima are given in Figures 1 and 2 in the main text.

## SAPT0 energies for sandwich geometries of benzene-chelate and chelate-chelate stacking

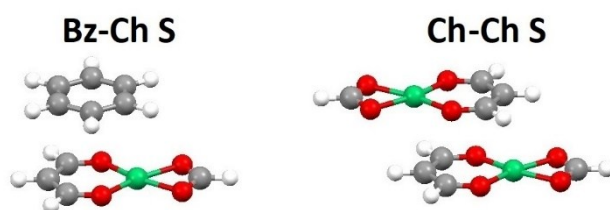


**Figure S3.** Sandwich geometries for benzene-chelate and chelate-chelate stacking of *acac*-type chelates

**Table S1.** Geometrical parameters (offset  $r$  and normal distance  $R$ ) and interaction energies (in kcal/mol) calculated at DFT-D and SAPT0 levels for sandwich geometries (**Bz-Ch S**, and **Ch-Ch S**, Figure S3) of *acac*-type benzene-chelate and chelate-chelate stacking. The SAPT0 energies consist of electrostatic (ELST), dispersion (DISP), exchange (EXCH) and induction component (IND). The sum of dispersion and exchange components is usually regarded as net dispersion (DISP + EXCH = NET DISP).<sup>3,4</sup>

<i>acac</i> Bz-Ch S	$r$ [Å]	$R$ [Å]	$\omega$ B97X-D/ def2-TZVP <sup>a</sup>	SAPT0/ def2-TZVP	ELST	DISP	EXCH	IND	NET DISP
Ni	0.0	3.52	-4.49	-4.77	-3.41	-7.79	+7.01	-0.57	-0.78
Cu	0.0	3.49	-4.99	-5.24	-4.02	-8.08	+7.61	-0.76	-0.47
Zn	0.0	3.46	-5.49	-5.55	-4.53	-8.32	+8.30	-0.99	-0.02
<i>acac</i> Ch-Ch S	$r$ [Å]	$R$ [Å]	LC- $\omega$ PBE-D3BJ/ aug-cc-pVDZ <sup>b</sup>	SAPT0/ def2-TZVP	ELST	DISP	EXCH	IND	NET DISP
Ni	0.0	3.15	-8.95	-10.07	-11.75	-11.08	+14.31	-1.55	+3.23
Cu	0.0	3.05	-10.96	-12.21	-15.35	-12.61	+18.63	-2.88	+6.02
Zn	0.0	2.93	-13.20	-14.70	-20.73	-14.64	+25.99	-5.31	+11.35

<sup>a</sup>  $\omega$ B97X-D is in good agreement with CCSD(T)/CBS for benzene-chelate stacking;<sup>1</sup> <sup>b</sup> LC- $\omega$ PBE-D3BJ/aug-cc-pVDZ is in good agreement with CCSD(T)/CBS for chelate-chelate stacking<sup>5</sup>

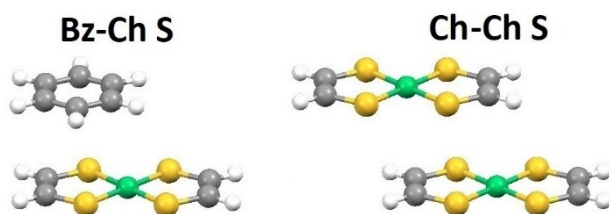


**Figure S4.** Sandwich geometries for benzene-chelate and chelate-chelate stacking of Ni dithiolene chelates

**Table S2.** Geometrical parameters (offset  $r$  and normal distance  $R$ ) and interaction energies (in kcal/mol) calculated at DFT-D and SAPTO levels for benzene-chelate (Bz-Ch) and chelate-chelate (Ch-Ch) stacking of Ni dithiolene (*dt*) chelate (Figure S4).

Ni <i>dt</i>	$r$ [Å]	$R$ [Å]	DFT-D <sup>a</sup>	SAPTO/ cc-pVDZ	ELST	DISP	EXCH	IND	NET DISP
Bz-Ch S	0.0	3.76	-3.92	-4.18	-2.59	-8.31	+7.47	-0.74	-0.84
Ch-Ch S	0.0	3.73	-7.23	-8.03	-4.83	-13.00	+11.10	-1.31	-1.90

<sup>a</sup>  $\omega$ B97X-D/6-31+G\* was used for benzene-chelate and PBE0-D3BJ/6-31G\* for chelate-chelate stacking, since they are in good agreement with CCSD(T)/CBS energies<sup>2</sup>

## SAPT2 and SAPT2+3 energies for stacking of benzene with *acac*-type chelates

**Table S3.** Geometrical parameters (offset *r* and normal distance *R*) and interaction energies (in kcal/mol) calculated at  $\omega$ B97X-D\* and **SAPT2** levels for the benzene-chelate sandwich geometry (**Bz-Ch S**, Figure S3) and minima at benzene-chelate potential energy curves (**Bz-Ch min1** and **Bz-Ch min2**, Figure 1 in the main text) for chelate-benzene stacking. The SAPT2 energies consist of electrostatic (ELST), dispersion (DISP), exchange (EXCH) and induction component (IND). The sum of dispersion and exchange components is usually regarded as net dispersion (DISP + EXCH = NET DISP). SAPT2 is not applicable for open-shell systems, as is the [Cu(CHO<sub>2</sub>)(C<sub>3</sub>H<sub>3</sub>O<sub>2</sub>)] complex studied in this work.

<b>Bz-Ch min1</b>	<i>r</i> [Å]	<i>R</i> [Å]	$\omega$ B97X-D**	SAPT2**	ELST	DISP	EXCH	IND	NET DISP
Ni	1.3	3.40	-4.82	-4.75	-3.44	-8.06	+7.57	-0.82	-0.49
Cu	1.2	3.40	-4.92	-	-	-	-	-	-
Zn	1.0	3.43	-4.93	-4.82	-3.50	-8.09	+7.61	-0.84	-0.48
<b>Bz-Ch S</b>	<i>r</i> [Å]	<i>R</i> [Å]	$\omega$ B97X-D**	SAPT2**	ELST	DISP	EXCH	IND	NET DISP
Ni	0.0	3.52	-4.49	-4.27	-3.11	-7.79	+7.20	-0.57	-0.59
Cu	0.0	3.49	-4.99	-	-	-	-	-	-
Zn	0.0	3.46	-5.49	-5.18	-4.27	-8.32	+8.39	-0.97	+0.07
<b>Bz-Ch min2</b>	<i>r</i> [Å]	<i>R</i> [Å]	$\omega$ B97X-D**	SAPT2**	ELST	DISP	EXCH	IND	NET DISP
Ni	1.4	3.37	-5.52	-5.18	-3.96	-9.00	+8.60	-0.82	-0.40
Cu	1.3	3.31	-6.43	-	-	-	-	-	-
Zn	1.3	3.27	-7.56	-6.97	-6.37	-10.12	+11.15	-1.64	+1.03

\*  $\omega$ B97X-D is in good agreement with CCSD(T)/CBS for chelate-aryl stacking of *acac*-type chelates<sup>1</sup>

\*\* def2-TZVP basis set

**Table S4.** Geometrical parameters (offset *r* and normal distance *R*) and interaction energies (in kcal/mol) calculated at  $\omega$ B97X-D\* and **SAPT2+3** levels for the benzene-chelate sandwich geometry (**Bz-Ch S**, Figure S3) and minima at benzene-chelate potential energy curves (**Bz-Ch min1** and **Bz-Ch min2**, Figure 1 in the main text) for chelate-benzene stacking. SAPT2+3 is not applicable for open-shell systems, as is the [Cu(CHO<sub>2</sub>)(C<sub>3</sub>H<sub>3</sub>O<sub>2</sub>)] complex studied in this work.

<b>Bz-Ch min1</b>	<i>r</i> [Å]	<i>R</i> [Å]	$\omega$ B97X-D**	SAPT2+3**	ELST	DISP	EXCH	IND	NET DISP
Ni	1.3	3.40	-4.82	-3.94	-3.27	-7.43	+7.57	-0.82	+0.14
Cu	1.2	3.40	-4.92	-	-	-	-	-	-
Zn	1.0	3.43	-4.93	-4.03	-3.35	-7.45	+7.61	-0.84	+0.16
<b>Bz-Ch S</b>	<i>r</i> [Å]	<i>R</i> [Å]	$\omega$ B97X-D**	SAPT2+3**	ELST	DISP	EXCH	IND	NET DISP
Ni	0.0	3.52	-4.49	-3.89	-3.06	-7.47	+7.20	-0.57	-0.27
Cu	0.0	3.49	-4.99	-	-	-	-	-	-
Zn	0.0	3.46	-5.49	-4.58	-4.11	-7.89	+8.39	-0.97	+0.50
<b>Bz-Ch min2</b>	<i>r</i> [Å]	<i>R</i> [Å]	$\omega$ B97X-D**	SAPT2+3**	ELST	DISP	EXCH	IND	NET DISP
Ni	1.4	3.37	-5.52	-5.03	-3.85	-8.96	+8.60	-0.82	-0.36
Cu	1.3	3.31	-6.43	-	-	-	-	-	-
Zn	1.3	3.27	-7.56	-6.46	-6.03	-9.94	+11.15	-1.64	+1.21

\*  $\omega$ B97X-D is in good agreement with CCSD(T)/CBS for chelate-aryl stacking of *acac*-type chelates<sup>1</sup>

\*\* def2-TZVP basis set

## SAPT2 and SAPT2+3 energies for stacking of benzene and *dt* chelate of nickel

**Table S5.** Geometrical parameters (offset *r* and normal distance *R*) and interaction energies (in kcal/mol) calculated at  $\omega$ B97X-D\* and **SAPT2** levels for benzene-chelate sandwich geometry (**Bz-Ch S**, Figure S4) and minima at benzene-chelate potential energy curves (**Bz-Ch min1** and **Bz-Ch min2**, Figure 2 in the main text) for the stacking of Ni dithiolene (*dt*) chelate with benzene.

Ni <i>dt</i> Bz-Ch	<i>r</i> [Å]	<i>R</i> [Å]	$\omega$ B97X-D**	SAPT2***	ELST	DISP	EXCH	IND	NET DISP
min1	1.5	3.50	-4.78	-4.45	-3.48	-7.98	+8.24	-1.22	+0.26
S	0.0	3.76	-3.92	-3.48	-2.00	-8.31	+7.57	-0.74	-0.74
min2	1.8	3.61	-5.43	-4.89	-3.58	-11.62	+11.83	-1.52	+0.21

\*  $\omega$ B97X-D is in good agreement with CCSD(T)/CBS for chelate-aryl stacking of Ni *dt* chelate <sup>2</sup>

\*\* 6-31+G\* basis set

\*\*\* cc-pVDZ basis set

**Table S6.** Geometrical parameters (offset *r* and normal distance *R*) and interaction energies (in kcal/mol) calculated at  $\omega$ B97X-D\* and **SAPT2+3** levels for benzene-chelate sandwich geometry (**Bz-Ch S**, Figure S4) and minima at benzene-chelate potential energy curves (**Bz-Ch min1** and **Bz-Ch min2**, Figure 2 in the main text) for the stacking of Ni dithiolene (*dt*) chelate with benzene.

Ni <i>dt</i> Bz-Ch	<i>r</i> [Å]	<i>R</i> [Å]	$\omega$ B97X-D**	SAPT2+3***	ELST	DISP	EXCH	IND	NET DISP
min1	1.5	3.50	-4.78	-3.21	-3.47	-6.75	+8.24	-1.22	+1.49
S	0.0	3.76	-3.92	-2.88	-2.59	-7.12	+7.57	-0.74	+0.45
min2	1.8	3.61	-5.43	-4.29	-4.61	-9.98	+11.83	-1.53	+1.85

\*  $\omega$ B97X-D is in good agreement with CCSD(T)/CBS for chelate-aryl stacking of Ni *dt* chelate <sup>2</sup>

\*\* 6-31+G\* basis set

\*\*\* cc-pVDZ basis set

## Potential energy curves for chelate-chelate stacking

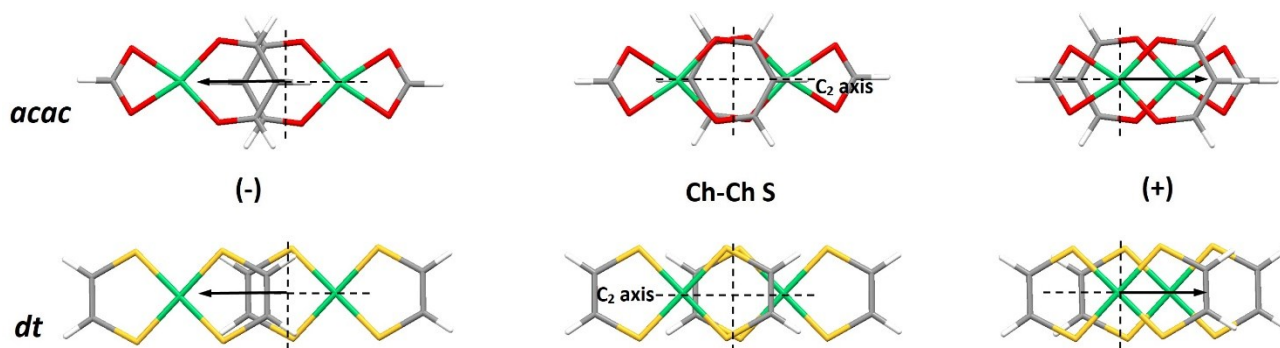


**Figure S5.** In the chelate-chelate sandwich geometry (**Ch-Ch S**) center of one chelate ring is exactly above the center of the other chelate ring. The potential surfaces are calculated by varying the normal distances for the series of offset values. In all calculations the interplanar angle between the rings is 0°. For the *acac* chelates, the offsets are denoted negative (-) if metals are moving away from each other, and positive (+) if metals are moving closer to each other.<sup>5</sup> For dithiolene (*dt*) chelates, negative and positive offsets are equivalent.<sup>2</sup>

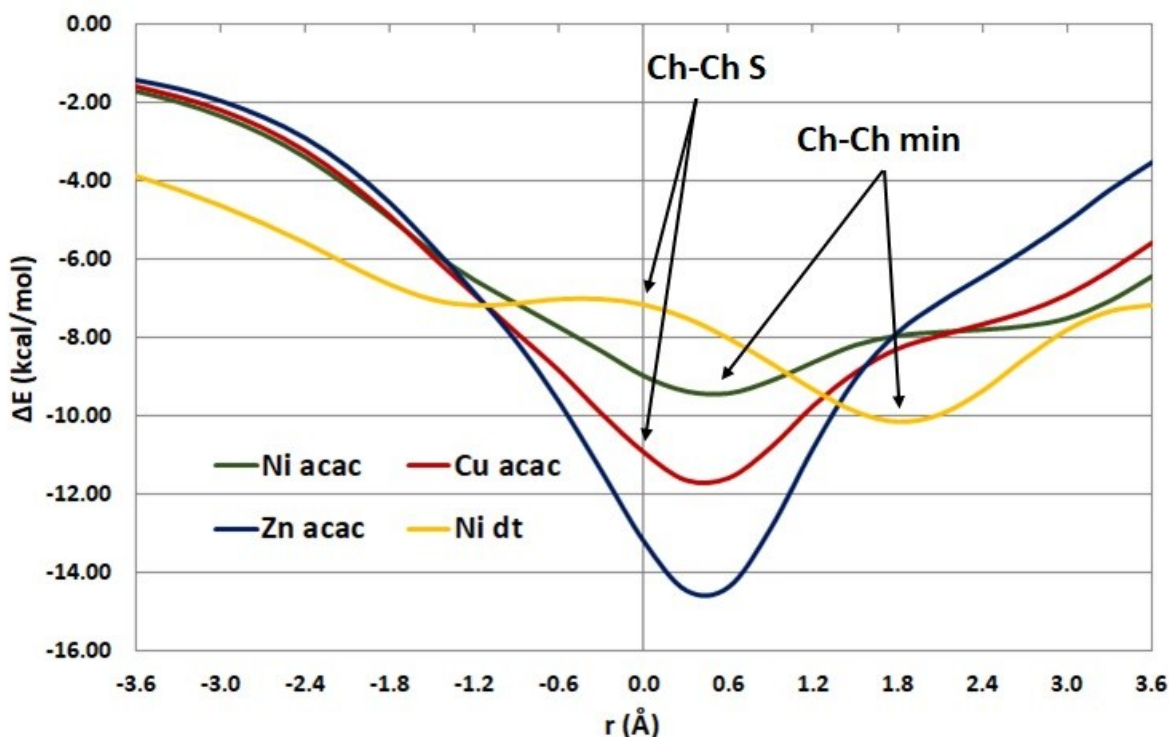


**Figure S6.** Potential energy curves for chelate-chelate stacking calculated at LC- $\omega$ PBE-D3BJ/aug-cc-pVDZ level for Ni *acac*-type chelates<sup>5</sup> and at PBE0-D3BJ/6-31G\* level for Ni dithiolene (*dt*) chelates.<sup>2</sup> The curves were obtained by varying the normal distances for a series of offset values and they show the energies of the strongest interactions for all offsets. The geometries of the minima are given in Figures 1 and 2 in the main text.

## SAPT2 energies for chelate-chelate stacking

**Table S7.** Geometrical parameters (offset **r** and normal distance **R**) and interaction energies (in kcal/mol) calculated at LC- $\omega$ PBE-D3BJ\* and SAPT2 levels for the chelate-chelate sandwich geometry (**Ch-Ch S**, Figure S3) and minimum at chelate-chelate potential energy curves (**Ch-Ch min**, Figure 1 in the main text) for *acac*-type chelate-chelate stacking. SAPT2 is not applicable for open-shell systems, as is the [Cu(CHO<sub>2</sub>)(C<sub>3</sub>H<sub>3</sub>O<sub>2</sub>)] complex studied in this work.

Ch-Ch S	r [Å]	R [Å]	LC- $\omega$ PBE-D3BJ**	SAPT2***	ELST	DISP	EXCH	IND	NET DISP
Ni	0.0	3.15	-8.95	-6.35	-10.42	-10.08	+16.75	-1.60	+5.67
Cu	0.0	3.05	-10.96	-	-	-	-	-	-
Zn	0.0	2.93	-13.20	-9.36	-18.55	-14.64	+29.29	-5.46	+14.65
Ch-Ch min	r [Å]	R [Å]	LC- $\omega$ PBE-D3BJ**	SAPT2***	ELST	DISP	EXCH	IND	NET DISP
Ni	0.5	3.13	-9.47	-6.67	-11.27	-11.89	+18.35	-1.86	+6.46
Cu	0.4	3.01	-11.70	-	-	-	-	-	-
Zn	0.4	2.88	-14.58	-10.06	-21.59	-16.18	+34.52	-6.81	+18.34

\* LC- $\omega$ PBE-D3BJ is in good agreement with CCSD(T)/CBS for *acac*-type chelate-chelate stacking<sup>5</sup>

\*\* aug-cc-pVDZ basis set

\*\*\* def2-TZVP basis set

**Table S8.** Geometrical parameters (offset **r** and normal distance **R**) and interaction energies (in kcal/mol) calculated at PBE0-D3BJ\* and SAPT2 levels for the chelate-chelate sandwich geometry (**Ch-Ch S**, Figure S3) and minimum at chelate-chelate potential energy curves (**Ch-Ch min**, Figure 2 in the main text) for Ni dithiolene (*dt*) chelate-chelate stacking.

Ni <i>dt</i> Ch-Ch	r [Å]	R [Å]	PBE0-D3BJ**	SAPT2***	ELST	DISP	EXCH	IND	NET DISP
Ch-Ch S	0.0	3.73	-7.23	-7.84	-5.04	-13.00	+11.52	-1.32	-1.48
Ch-Ch min	1.8	3.61	-10.14	-11.87	-8.45	-21.24	+21.31	-3.48	+0.07

\* PBE0-D3BJ is in good agreement with CCSD(T)/CBS for Ni dithiolene (*dt*) chelate-chelate stacking<sup>2</sup>

\*\* 6-31G\* basis set

\*\*\* cc-pVDZ basis set



## REFERENCES

- 1 D. P. Malenov, D. B. Ninković, D. N. Sredojević and S. D. Zarić, *ChemPhysChem*, 2014, **15**, 2458–2461.
- 2 D. P. Malenov, D. Ž. Veljković, M. B. Hall, E. N. Brothers and S. D. Zarić, *Phys. Chem. Chem. Phys.*, 2019, **21**, 1198–1206.
- 3 E. G. Hohenstein and C. D. Sherrill, *J. Phys. Chem. A*, 2009, **113**, 878–886.
- 4 C. D. Sherrill, *Acc. Chem. Res.*, 2013, **46**, 1020–1028.
- 5 D. P. Malenov and S. D. Zarić, *Phys. Chem. Chem. Phys.*, 2018, **20**, 14053–14060.